frontiers in Materials

ORIGINAL RESEARCH
published: 17 December 2021
doi: 10.3389/fmats.2021.792768

Study on the Soft Magnetic Properties of FeSiB/EP Composites by Direct Ink Writing

Ma Qing[1], *Teng Chong*[1], *Hu Jing*[1]* *and Baoan Sun*[2]

[1]*Beijing Key Laboratory of Quality Evaluation Technology for Hygiene and Safety of Plastics, School of Chemistry and Materials Engineering, Beijing Technology and Business University, Beijing, China,* [2]*Songshan Lake Materials Laboratory, Dongguan, China*

Fe-based amorphous alloy has excellent soft magnetic properties; traditionally, Fe-based amorphous alloy such as soft magnetic devices was fabricated by insulation enveloping and suppression molding methods. In this process, the aging of organic envelope materials and the crystallization of Fe-based amorphous alloy were usually occurring, accompanying with low magnetic induction and poor mechanical properties. The direct ink writing (DIW) technique can make complex-shaped parts and needs no heating treatment after forming, which can avoid the effect of traditional molding process. In the present study, varying mass fraction FeSiB/EP composite parts were prepared by the DIW technique with the Fe-based amorphous alloy powder and epoxy resin, in which microscopic morphology, magnetic properties, and mechanical properties of FeSiB/EP soft magnetic composites were studied. The results indicate that the slurry with iron powder mass fraction of 92.3, 92.6, and 92.8 wt% has good printing performance and self-support ability, which is suitable for DIW. The density of the printed parts is about 4.317, 4.449, and 4.537 g/cm^3, which is almost similar with the iron powder. The tensile strength and elongation of printing parts are significantly improved compared with the pure epoxy resin. From the photos of microscopic morphology of printing parts, it can be seen that FeSiB powders are evenly dispersed in EP, no pores, and defects, with the proportion increasing of powders; the insulation coating thickness decreases; and the magnetic performance improves. The optimal sample is 92.8 wt% FeSiB/EP, in which saturation magnetic induction strength is 137.9759 emu/g and coercivity is 4.6523 A/m.

Keywords: fe-based amorphous alloy, direct ink writing technique, SMC, magnetic performance, rheological behavior

OPEN ACCESS

Edited by:
Jiang Ma,
Shenzhen University, China

Reviewed by:
Juntao Huo,
Ningbo Institute of Materials Technology and Engineering (CAS), China
Yu Wang,
University of Science and Technology of China, China

***Correspondence:**
Hu Jing
hujing@th.btbu.edu.cn

Specialty section:
This article was submitted to Ceramics and Glass, a section of the journal Frontiers in Materials

Received: *11 October 2021*
Accepted: *08 November 2021*
Published: *17 December 2021*

Citation:
Qing M, Chong T, Jing H and Sun B (2021) Study on the Soft Magnetic Properties of FeSiB/EP Composites by Direct Ink Writing. Front. Mater. 8:792768. doi: 10.3389/fmats.2021.792768

1 INTRODUCTION

Soft magnetic composites (SMCs) were composed of ferromagnetic phase and insulation coating; the ferromagnetic phase was embedded in an insulating matrix (Shokrollahi and Janghorban,2007). The resulted materials present a unique set of properties such as low eddy current losses at medium to high frequencies, high saturation induction, relatively high magnetic permeability, low coercivity, and isotropy of physical properties (Shokrollahi and Janghorban,2007; Sunday and Taheri, 2017). With the demand of high-frequency motor, 5G communication, etc., it becomes a noticeable topic to develop SMCs combined with high saturated magnetization value (Ms), low coercivity (Hc), low core loss, and low materials cost. The traditional SMCs could not meet the above requirements anymore. However, Fe-based amorphous alloy showed excellent soft magnetic properties, there was no

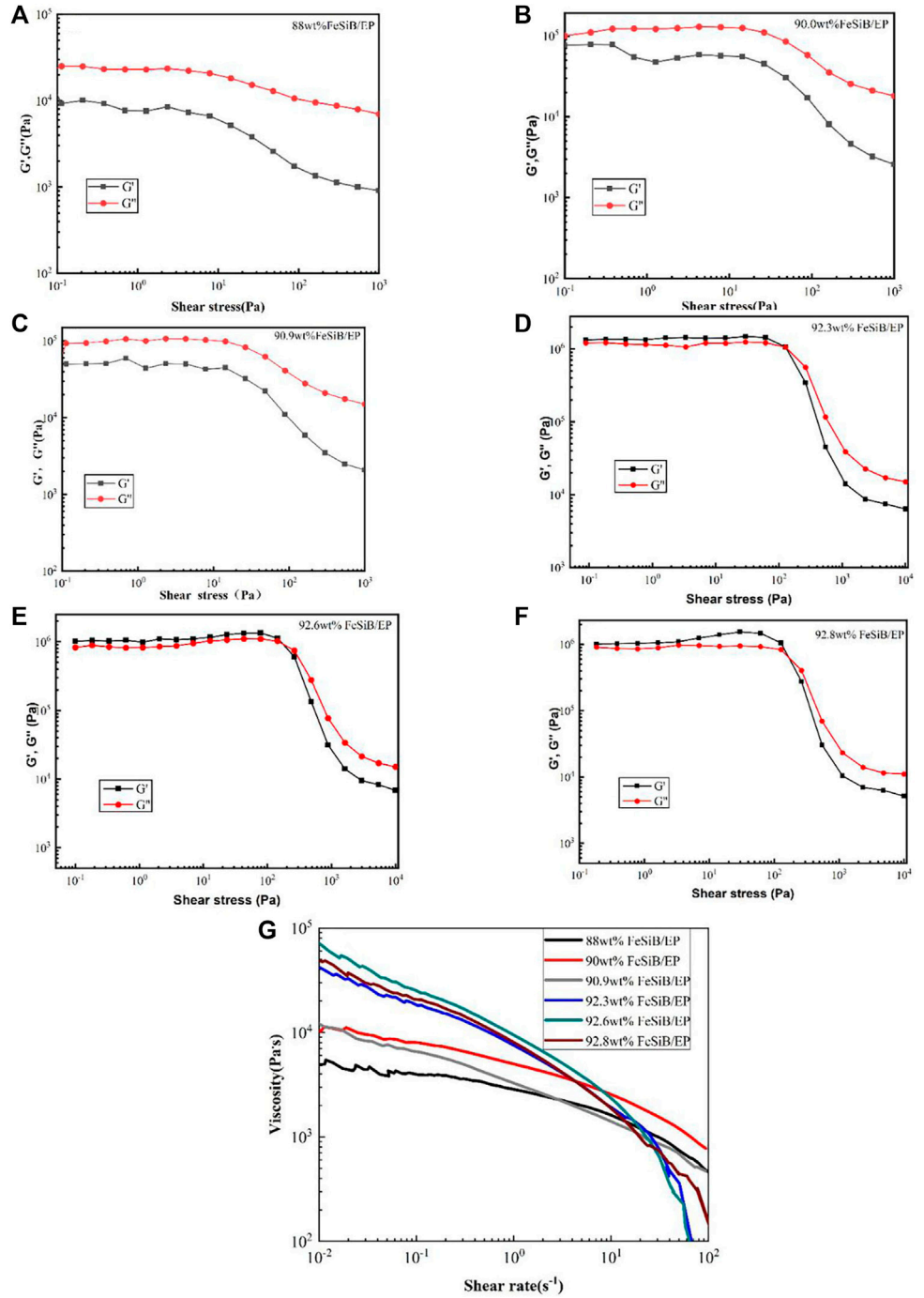

FIGURE 1 | (A–F) Shear storage modulus (G′) and loss modulus (G″) of epoxy-based slurry with varying compositions as a function of shear stress and **(G)** viscosity curves as a function of shear rate.

magnetic anisotropy caused by crystal structure, and its curie point was much lower than crystal soft magnetic material; therefore, it could greatly reduce eddy currents and diminish their total energy losses (Wang et al., 2016). As it is well known, limited by the ability of amorphous formation, Fe-based amorphous alloy was usually in powder form, so the powder metallurgy method was used to make soft magnetic device, but the possible crystallization in post-processing was an inevitable defect of this processing method (Luo et al., 2021; Vijayakumar et al., 2021).

Three-dimensional (3D) printing technologies were attempted to be applied; laser solid forming, selective laser melting, and laser

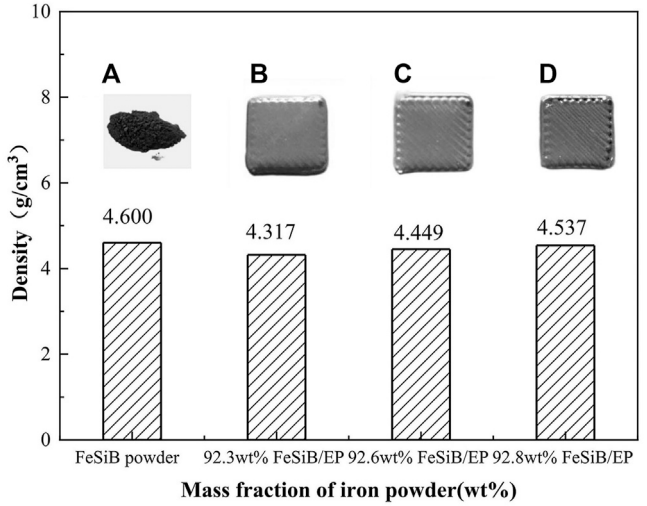

FIGURE 2 | The density of printing parts and the photos of printing samples with different iron powder content: **(A)** FeSiB powder, **(B)** 92.3 wt% FeSiB/EP, **(C)** 92.6 wt% FeSiB/EP, and **(D)** 92.8 wt% FeSiB/EP

rapid prototyping were used mostly (Yang et al., 2012; Pauly et al., 2013; Sahasrabudhe et al., 2013). During this process, the forming of heat-affected zone was also a defect of possible crystallization (Lin et al., 2019; Wu et al., 2019). Another attractive 3D processing was the direct ink writing (DIW), the most obvious feature of this technology was that it was printed on the basis of extruded concentrated slurry (Truby and Lewis, 2016), so long as the material that could be adjusted into slurry could be formed in DIW, such as polymer slurry (Zhang et al., 2021a), metal slurry, and cell slurry (Yuk and Zhao, 2018). It had also been studied to process magnetic materials, Fe-based metallic glass slurries were printed with DIW in the work Wu et al. (Wu et al., 2018), and alkaline environment was not conducive to the wetting and stable dispersion. Amir et al. evaluated DIW as a technique for creating parts using nickel-based superalloy 625, which maintain high fatigue resistance (Mostafaei et al., 2018). Hong et al. systematically studied and modified the Fe-Mn alloy composition to achieve the enhanced degradation rates by using the DIW technique (Hong et al., 2016).

There were eddy current loss and iron consumption that display in Fe-based amorphous alloy and other Ferromagnetic material (Li et al., 2019). In the past work, the insulation coatings were used to reduce eddy losses and improve magnetism, such as SiO_2 (Zhou et al., 2020), phosphate-polyimide insulating layer (Chen et al., 2020), and magnesium alloy (Zhang et al., 2021b). In the recent years, a SiO_2 ceramic material had been used as an insulation coating in the preparation of SMCs due to its excellent chemical inertness, excellent heat resistance, and high resistivity. However, the high effective permeability (μ_e) of the FeSiBCC@SiO_2 decreased monotonically with increasing thickness of the SiO_2 coating (Zhou et al., 2020). Chen et al. (Chen et al., 2020) demonstrated that, when iron-based SMCs were coated with phosphate-polyimide (0.1 wt% phosphoric acid and 1.5 wt% polyimide), the corrosion resistance of the sample was significantly improved. However, the core loss of the SMCs was 186.6 mW/g, and their soft magnetic performance was deteriorated. Fe/Fe_3O_4/silicon resin SMCs had a high saturated magnetization value (201 Am^2 kg^{-1}) and relatively high coercivity (11.4 Oe) (Meng et al., 2020). Another type of insulating coating short Fe fibers was added to the polymer to insulate and hinder the eddy currents. Nevertheless, the electrical resistivity had large core losses, especially at a higher frequency (Neamțu et al., 2020). Ren et al. fabricated the (Fe@Fe_xO_y)/epoxy resin (ER) composites and acquired the high-performance electromagnetic insulating materials, but the ER coating was decomposed when the heat treatment temperature was too high or the time was too long (Ren et al., 2015; Wang et al., 2021). ER is an organic insulation material; room temperature is viscous liquid, mixed with iron-based amorphous powder very suitable for direct writing at room temperature molding.

In the current study, FeSiB/EP composite parts were successfully fabricated by DIW. The rheological behavior of FeSiB/EP slurry was deeply investigated. The microstructural evolution of the FeSiB/EP composites and the density of FeSiB/EP composites were also explored. Besides, the effects of magnetic performance and mechanical properties of FeSiB/EP composites were also studied. Our results show that the coercivity of FeSiB/EP composites was decreased, and eddy currents were also diminished. Meanwhile, the composites remain mechanical and saturation magnetic induction strength good enough as well.

2 MATERIALS AND METHODS

2.1 Materials

A bisphenol-A ER E-44 with an epoxy value of 0.41–0.47 was purchased from Shanghai Licheng Adhesive Co., Ltd., Shanghai, China. The curing agents were polyamide curing agent, which were supplied by Shanghai Licheng adhesive Co., Ltd., Shanghai, China. FeSiB amorphous alloy powder, with particle size of 25 μm, was provided by Advanced Technology and Materials Co., Ltd., Beijing, China.

2.2 Preparation of FeSiB/Epoxy Composite Slurry and Printing Parts

The weight ratio of ER to polyamide curing agent was 1:1. The iron-based amorphous alloy powder was added to mixture and stirred for 2 min, so that the blend was thoroughly stirred. The weight percentage of the added FeSiB was 88.0, 90.0, 90.9, 92.3, 92.6, and 92.8 wt%.

The prepared slurry was put into the printing cartridge; the nozzle diameter was 0.6 mm. Processing parameters were set as follows: the printing speed is 1 mm/s; the printing pressure is 95 psi; the height of layer is 0.4 mm; and the spacing is 0.6 mm. The printed parts were absolutely cured after 24 h at room temperature.

2.3 Characterizations

2.3.1 Rheological Behavior Measurement

Rheological properties of the composite slurry were characterized using a rheometer (HAAKE MARSIII, Thermo Fisher Scientific

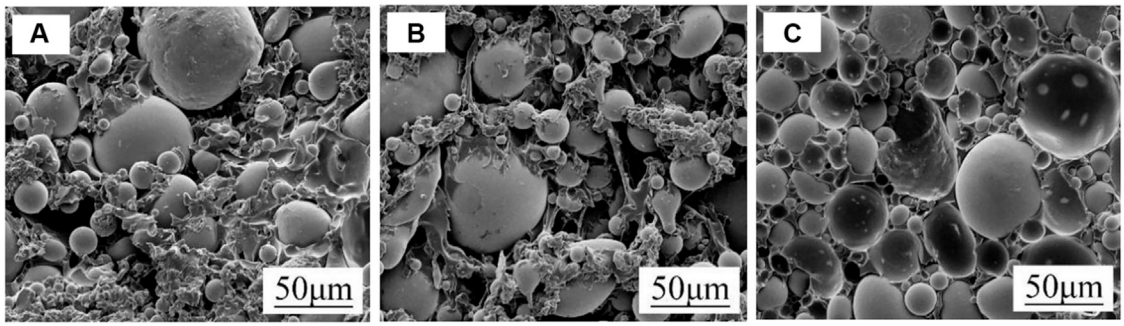

FIGURE 3 | SEM image of cross sections with different iron powder content: **(A)** 92.3 wt% FeSiB **(B),** 92.6 wt% FeSiB, and **(C)** 92.8 wt% FeSiB.

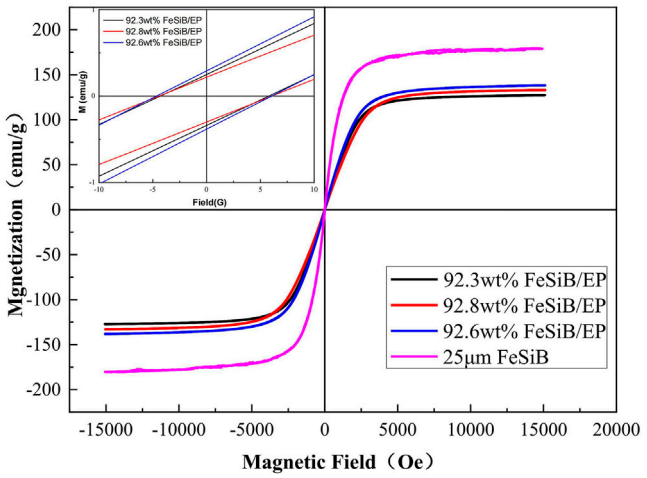

FIGURE 4 | Hysteresis circuit diagram of FeSiB/EP printed samples.

Inc., United States) with a 20-mm flat plate and a gap of 0.5 mm. Frequency was set to 1.0 Hz under scanning in oscillation mode at 25°C. When we tested the modulus, the scan mode was set as stress logarithmic scan, and the scan range was 0.1–10,000 Pa. When we obtained dynamic viscosity, the scan model was selected shear rate logarithmic scanning mode. The shear rate was increased from 0.01 to 100 s^{-1}.

2.3.2 Density Test

The parts density was measured using the Archimedes' principle (CPA2245, Sartorius Scientific Instruments Ltd., Beijing).

$$m_e g = m_h g + \rho_h g V_p \tag{2.1}$$

$$m_e = m_h + \rho_h \frac{m_e}{\rho} \tag{2.2}$$

$$\rho = \frac{\rho_h m_e}{m_e - m_h} \tag{2.3}$$

In the formula, is the density of the object itself, is the density of the water, is the mass of the object in the air, and is the mass of the object in the water.

2.3.3 Scanning Electron Microscopy

The samples were cut in half and attached to a stub with conductive adhesive and then coated with 25 nm of gold using a sputter coater in nitrogenous atmosphere. The samples were scanned at 10^5–10 kV accelerating voltage using secondary electron detection to obtain the cross sections and surface images of the 3D printed parts (Phenom XL, Phenom China, Shanghai).

2.3.4 Magnetic Performance Test

The magnetic performance of the composites was measured at a frequency range of −1.5–1.5 T using a vibrational sample magnetometer (LakeShore7404, Linkphysics Corporation, Shanghai).

2.3.5 Mechanical Properties

Mechanical properties tests included the tensile strength and tensile elastic modulus of the spline, with standard tensile strips ISO527. Splines were tested on a omnipotence tensile tester (CMT6104, Shenzhen Xinsanisi Metrology Technology Co., Ltd., Shenzhen) with three average for each ratio. The rate of extension was 2 mm/min.

3 RESULTS AND DISCUSSION

3.1 Rheological Behavior Measurement

The rheological behaviors of FeSiB/epoxy composite slurry with different ratios are shown in **Figure 1**. G′ is the energy storage modulus, represents the elasticity of the slurry; G″ is the loss modulus, represents the viscosity of the slurry. As could be seen in **Figures 1A–C**, G′ was always lower than G″, and the slurry showed the fluid properties (Liu et al., 2020). These kinds of slurry flow readily through nozzle under modest applied pressure and then immediately wetted and spread upon when exiting the nozzle, so the ability to support themselves was lacking. From **Figures 1D–F**, when the shear stress was low, G′ and G″ curves of the slurry fluctuated slightly, G′ was always higher than G″, and the slurry showed solid properties. As the shear stress increased, the two curves intersected, the intersection was yield stress point of the slurry, and the yield stress increased with the growing of

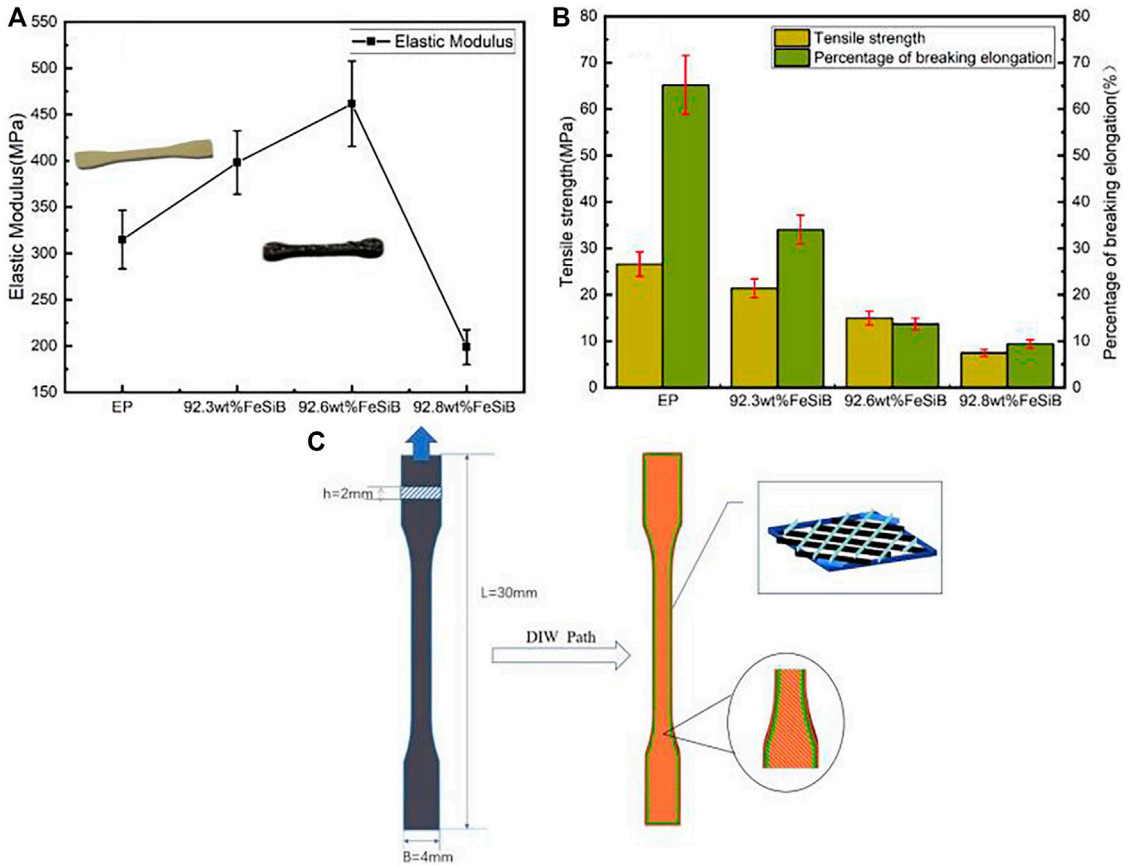

FIGURE 5 | (A) Elastic modulus of the samples with different mass ratios. **(B)** Tensile strength and fracture elongation of the samples with different mass ratios. **(C)** DIW path.

iron powder content. When the shear stress was greater than yield stress, the slurry showed the nature of liquid and indicated that the slurry was viscoelastic fluid with good printing and self-supporting performance. Comparing the viscosity of each mass ratio in **Figure 1G**, the viscosity of the slurry increased with Fe powder contents and decreased with shear rate and showed strong shear thinning behavior, which proved that the slurry had good printing performance (Guo, 2020).

3.2 Density Test

The different densities of 3D printing samples and their photos are shown in **Figure 2**. Density was an important factor affecting the magnetic performance. According to the test results, as the proportion of FeSiB powder contents was increased, the density of the sample increased too and was very closing to the powder density. From the photos, we could see that the surfaces were very smooth, and the printing tracks were clearer with the proportion of iron powder increasing. That means that the high proportion slurry had high printing accuracy.

3.3 Scanning Electron Microscopy

Figures 3A–C present the representative SEM images of the cross sections of 3D printing sample with different filler contents. The dark area was epoxy adhesive, and the bright area was the FeSiB particles. It is clear that there were not any obvious reunion phenomenon and uniform distribution of FeSiB powder. Pull phenomenon was also common in the section part of the sample, which was caused by the uneven distribution of the excess adhesive on the particle surface. As the proportion of the adhesive content decreased, the compatibility between the print layers was better, and there was no obvious separation interface, which provided a guarantee for the magnetic and mechanical property. With the proportion of FeSiB powder increased, the thickness of adhesive coating decreased, which was conducive to the improvement of magnetic performance. During printing, the slurry self-flows before curing, which could fill the gaps between the layers, giving the sample higher cohesiveness, and the toughness nest found indicated a certain bond strength in **Figure 3C**.

3.4 Magnetic Performance Test

As for soft magazine material, the higher saturated magnetization and lower coercivity were more suitable to be used in inductors, transformers, etc. **Figure 4** displays the hysteresis loops for the original FeSiB particles and the 3D printing samples with different mass ratios. All the four samples showed typical

single-phase magnetic hysteresis along with good intrinsic magnetism. FeSiB powder indicated a high saturated magnetization value (Ms = 179.164 emu/g) and a low coercivity (Hc = 5.6834 Oe). The three composite samples presented lower coercivity value of 4.2994 Oe for 92.3 wt% FeSiB/EP, 4.6523 Oe for 92.6 wt% FeSiB/EP, and 4.4105 Oe for 92.8 wt% FeSiB/EP, which might be ascribed to the uniform and completed resin coating of FeSiB particles; a small amount of ER decreased the coercivity of FeSiB/EP composite. From **Figure 4**, the three composite samples also demonstrated a relatively high saturated magnetization value of 127.98 emu/g for 92.3 wt% FeSiB/EP, 137.01 emu/g for 92.6 wt% FeSiB/EP, and 132.98 emu/g for 92.8 wt% FeSiB/EP. Their remanence of the samples was all very low. The saturated magnetization value of the composition was lower than that of FeSiB particles, because of the insulation of epoxy. From **Figure 4**, it could be seen that 92.6 wt% FeSiB/EP was the best comprehensive magnetic properties composite formula; as for the higher powder content, the amount of resin is reduced, the mixing uniformity with powder becomes difficulty, and it is easy to form holes locally and accumulate locally in other areas.

The non-uniformity of resin and holes affects the magnetic properties of printing parts.

3.5 Mechanical Properties

As shown in **Figure 5**, the tensile strength of pure epoxy by compression molding with 60°C was 26.59°MPa, and the break elongation was 65.19%. All were higher than splines containing different proportions of FeSiB. As the FeSiB mass ratio increased, the tensile strength and the break elongation reduced. Among them, the 92.3 wt% FeSiB/EP tensile strength was 21.39°MPa, closed proximity to pure epoxy, but its break elongation was 34.02%, fall by half compared with pure epoxy. This might be because the epoxy continuous phase was disrupted by FeSiB particles. However, the elastic modulus was up to 461.47 MPa for 92.6 wt% FeSiB/EP. The pure epoxy elastic modulus was 314.95 MPa. This showed that the stiffness significantly increased with the content of magnetic powder. While the content of magnetic powder continued to increase, the elastic modulus of the sample was reduced sharply. Hence, the tensile strength and the break elongation of the sample decreased with the FeSiB powder ratio, but the elastic modulus prominent increased.

4 CONCLUSION

Different mass ratios of 3D printing slurry were configured with iron-based amorphous alloy powder and ER. The rheological behavior of the slurry was measured by rheometer; it can be investigated that the slurry showed performance of liquid in lower shear stress and proved that the slurry had good printing performance and self-supporting performance, and when the shear stress was greater than its yield stress, the slurry showed the nature of solid. From the SEM imagines of the printing samples, we could see that the sample had a uniform microstructure and high density, and iron particles were evenly dispersed in the binder.

The coercivity of the three samples with different mass ratios was lower than that of the iron-based amorphous alloy powder, which showed that the introduction of ER was beneficial to reduce the coercivity, reduce the vortex loss, and improve the magnetic performance of FeSiB/EP composite materials. From the mechanics performance test, it can be seen that, as the proportion of adhesive was reduced, the stretch performance of the sample was decreasing, and the elastic modulus increased first and then decreased. Within all the samples, the iron powder of 92.6 wt% FeSiB/EP was demonstrated to be the optimum.

DATA AVAILABILITY STATEMENT

The raw data supporting the conclusion of this article will be made available by the authors, without undue reservation.

AUTHOR CONTRIBUTIONS

MQ is responsible for the experiment and thesis writing. TC is responsible for the test. HJ is responsible for the overall arrangement of the experiment and the revision of the paper.

REFERENCES

Chen, Y., Zhang, L., Sun, H., Chen, F., Zhang, P., Qu, X., et al. (2020). Enhanced Magnetic Properties of Iron-Based Soft Magnetic Composites with Phosphate-Polyimide Insulating Layer. *J. Alloys Compd.* 813, 152205. doi:10.1016/j.jallcom.2019.152205

Guo, Y. (2020). *Research on Preparation, Properties and Application of 3D Printing Nanocomposites*. Hefei, Anhui Province: University of Science and Technology of China.

Hong, D., Chou, D.-T., Velikokhatnyi, O. I., Roy, A., Lee, B., Swink, I., et al. (2016). Binder-jetting 3D Printing and alloy Development of New Biodegradable Fe-Mn-Ca/Mg Alloys. *Acta Biomater.* 45, 375–386. doi:10.1016/j.actbio.2016.08.032

Li, H. X., Lu, Z. C., Wang, S. L., Wu, Y., and Lu, Z. P. (2019). Fe-based Bulk Metallic Glasses: Glass Formation, Fabrication, Properties and Applications. *Prog. Mater. Sci.* 103, 235–318. doi:10.1016/j.pmatsci.2019.01.003

Lin, X., Zhang, Y., Yang, G., Gao, X., Hu, Q., Yu, J., et al. (2019). Microstructure and Compressive/tensile Characteristic of Large Size Zr-Based Bulk Metallic Glass Prepared by Laser Solid Forming. *J. Mater. Sci. Techn.* 35 (2), 328–335. doi:10.1016/j.jmst.2018.10.033

Liu, J., Guo, Y., Weng, C., Zhang, H., and Zhang, Z. (2020). High thermal Conductive Epoxy Based Composites Fabricated by Multi-Material Direct Ink Writing. *Compos. A: Appl. Sci. Manuf.* 129, 105684. doi:10.1016/j.compositesa.2019.105684

Luo, T., Zhang, H., Liu, R., Du, P., Huang, Z., Pan, Q., et al. (2021). Mechanical and Damping Properties of the Multi-Layer Graphenes Enhanced CrMnFeCoNi High-Entropy alloy Composites Produced by Powder Metallurgy. *Mater. Lett.* 293, 129682. doi:10.1016/j.matlet.2021.129682

Meng, B., Yang, B., Zhang, X., Zhou, B., Li, X., and Yu, R. (2020). Combinatorial Surface Coating and Greatly-Improved Soft Magnetic Performance of Fe/Fe3O4/resin Composites. *Mater. Chem. Phys.* 242, 122478. doi:10.1016/j.matchemphys.2019.122478

Mostafaei, A., Neelapu, S. H. V. R., Kisailus, C., Nath, L. M., Jacobs, T. D. B., and Chmielus, M. (2018). Characterizing Surface Finish and Fatigue Behavior in Binder-Jet 3D-Printed Nickel-Based Superalloy 625. *Addit. Manuf.* 24, 200–209. doi:10.1016/j.addma.2018.09.012

Neamțu, B. V., Irimie, A., Popa, F., Gabor, M. S., Marinca, T. F., and Chicinaș, I. (2020). Soft Magnetic Composites Based on Oriented Short Fe Fibres Coated with Polymer. *J. Alloys Compd.* 840, 155731. doi:10.1016/j.jallcom.2020.155731

Pauly, S., Löber, L., Petters, R., Stoica, M., Scudino, S., Kühn, U., et al. (2013). Processing Metallic Glasses by Selective Laser Melting. *Mater. Today* 16 (1-2), 37–41. doi:10.1016/j.mattod.2013.01.018

Ren, L., Zhao, J., Wang, S.-J., Han, B.-Z., and Dang, Z.-M. (2015). Dielectric and Magnetic Properties of Fe@FexOy/epoxy Resin Nanocomposites as High-Performance Electromagnetic Insulating Materials. *Compos. Sci. Techn.* 114, 57–63. doi:10.1016/j.compscitech.2015.04.003

Sahasrabudhe, H., Dittrick, S. A., and Bandyopadhyay, A. (2013). Laser Processing of Fe-Based Bulk Amorphous Alloy Coatings on Titanium. *Metall. Mat Trans. A.* 44 (11), 4914–4926. doi:10.1007/s11661-013-1846-0

Shokrollahi, H., and Janghorban, K. (2007). Soft Magnetic Composite Materials (SMCs). *J. Mater. Process. Techn.* 189 (1-3), 1–12. doi:10.1016/j.jmatprotec.2007.02.034

Sunday, K. J., and Taheri, M. L. (2017). Soft Magnetic Composites: Recent Advancements in the Technology. *Metal Powder Rep.* 72 (6), 425–429. doi:10.1016/j.mprp.2016.08.003

Truby, R. L., and Lewis, J. A. (2016). Printing Soft Matter in Three Dimensions. *Nature* 540 (7633), 371–378. doi:10.1038/nature21003

Vijayakumar, K., Thiagarajan, Y., Rajendirakumar, R., Joseph Basanth, A., Karthikeyan, R., and Kannan, S. (2021). Development of an Iron Powder Metallurgy Soft Magnetic Composite Core Switched Reluctance Motor. *Mater. Today Proc.* 41, 1195–1201. doi:10.1016/j.matpr.2020.10.346

Wang, A., Zhao, C., He, A., Yue, S., Chang, C., Shen, B., et al. (2016). Development of FeNiNbSiBP Bulk Metallic Glassy Alloys with Excellent Magnetic Properties and High Glass Forming Ability Evaluated by Different Criterions. *Intermetallics* 71, 1–6. doi:10.1016/j.intermet.2015.11.009

Wang, F., Dong, Y., Chang, L., Pan, Y., Chi, Q., Gong, M., et al. (2021). High Performance of Fe-Based Soft Magnetic Composites Coated with Novel Nano-CaCO3/epoxy Nanocomposites Insulating Layer. *J. Solid State. Chem.* 304, 122634. doi:10.1016/j.jssc.2021.122634

Wu, H., Liang, L., Zeng, H., Lan, X., Du, J., Zhou, C., et al. (2019). Microstructure and Nanomechanical Properties of Zr-Based Bulk Metallic Glass Composites Fabricated by Laser Rapid Prototyping. *Mater. Sci. Eng. A* 765, 138306. doi:10.1016/j.msea.2019.138306

Wu, W., Du, H., Sui, H., Sun, B., Wang, B., Yu, Z., et al. (2018). Study of Printing Parameters of Pneumatic-Injection 3D Printing of Fe-Based Metallic Glass. *J. Non Cryst. Sol.* 489, 50–56. doi:10.1016/j.jnoncrysol.2018.03.027

Yang, G., Lin, X., Liu, F., Hu, Q., Ma, L., Li, J., et al. (2012). Laser Solid Forming Zr-Based Bulk Metallic Glass. *Intermetallics* 22, 110–115. doi:10.1016/j.intermet.2011.10.008

Yuk, H., and Zhao, X. (2018). A New 3D Printing Strategy by Harnessing Deformation, Instability, and Fracture of Viscoelastic Inks. *Adv. Mater.* 30 (6), 1704028. doi:10.1002/adma.201704028

Zhang, B., Chung, S. H., Barker, S., Craig, D., Narayan, R. J., and Huang, J. (2021a). Direct Ink Writing of Polycaprolactone/Polyethylene Oxide Based 3D Constructs. *Prog. Nat. Sci. Mater. Int.* 31 (2), 180–191. doi:10.1016/j.pnsc.2020.10.001

Zhang, H., Wang, S., Yang, X., Hao, S., Chen, Y., Li, H., et al. (2021b). Interfacial Characteristic and Microstructure of Fe-Based Amorphous Coating on Magnesium alloy. *Surf. Coat. Techn.* 425, 127659. doi:10.1016/j.surfcoat.2021.127659

Zhou, B., Dong, Y., Chi, Q., Zhang, Y., Chang, L., Gong, M., et al. (2020). Fe-based Amorphous Soft Magnetic Composites with SiO2 Insulation Coatings: A Study on Coatings Thickness, Microstructure and Magnetic Properties. *Ceramics Int.* 46 (9), 13449–13459. doi:10.1016/j.ceramint.2020.02.128

Conflict of Interest: The authors declare that the research was conducted in the absence of any commercial or financial relationships that could be construed as a potential conflict of interest.

Publisher's Note: All claims expressed in this article are solely those of the authors and do not necessarily represent those of their affiliated organizations or those of the publisher, the editors, and the reviewers. Any product that may be evaluated in this article, or claim that may be made by its manufacturer, is not guaranteed or endorsed by the publisher.